Available online at www.sciencedirect.com
ScienceDirect
Talanta 70 (2006) 485–488
Talanta
www.elsevier.com/locate/talanta

An optical biosensor for kinetic analysis of soluble Interleukin-1 receptor I binding to immobilized Interleukin-1α

Bao-yan Wu, Yan-yan Wang, Jing Li, Zhao Song, Jia-dong Huang, Xin-sheng Wang, Qiang Chen *

College of Life Sciences, Nankai University, Tianjin 300071, China

Received 11 July 2005; received in revised form 11 December 2005; accepted 11 December 2005
Available online 19 January 2006

Abstract

We report here the development of an optical biosensor based on the resonant mirror for kinetic analysis of soluble Interleukin-1 receptor I (sIL-1R I) in solution binding to immobilized Interleukin-1α (IL-1α). IL-1α was immobilized through its surface amine groups via amide bonds with the carboxyl groups of the carboxymethyl dextran (CMD) on cuvette surface. The interaction of sIL-1R I and IL-1α was monitored in real time. Evaluation of the binding curves allowed the analysis of the binding kinetics. The linear range of sIL-1R I in solution was over a range of 100–1600 nM ($R = 0.9962$). Equilibrium dissociation constant (K_D) was derived by Scatchard plot analysis for sIL-1R I binding to immobilized IL-1α. For this assay, the K_D was 2.6×10^{-6} M. The CMD cuvette modified by IL-1α was successfully regenerated using 10 mM HCl, and the same sensing surface was used repeatedly for the interaction analysis.

Keywords: Optical biosensor; Kinetic analysis; Soluble Interleukin-1 receptor I; Interleukin-1α

Affinity interactions formation of biocomplexes including antigen–antibody, protein–nucleic acid, hybridization of complementary strands of ssDNA, chemoreceptor–ligand, drugs–ligand, represent the most important biochemical processes involved in nature [1,2]. Although typical enzyme-linked immunosorbent assay (ELISA) or other binding assays can yield valuable information about the binding affinity, they are usually allowed to reach equilibrium by use of a long incubation time, typically of several hours, and cannot measure in real time [3,4]. At present, the optical biosensor is considered as a convenient tool to detect chemicals or to investigate biomolecular affinity interaction [5]. Detection of a potential biospecific partner in either form of qualitative biosensor study leads logically to not only its isolation and identification but also the characterization of its function interaction in terms of reaction stoichiometry and equilibrium constant [6]. The binding analysis performed on the optical biosensor does not have to reach equilibrium, and carries out rapidly and conveniently, which allows real time monitoring of reaction, no requirement for radio-labeling or biochemical tagging, and reusability flexible experiment design, and rapid qualitative, quantitative, and kinetic information for the biomolecular interaction analysis [7,8]. A lot of studies for the optical biosensor have been reported in the field of chemical sensing, and medical chemistry [9–11]. The highly desirable potential of biosensor technology has led to the development of two classes of optical biosensor: the resonant mirror and surface plasmon resonance, which rely on somewhat different principles [12–14], which provide essentially equivalent opportunities for detecting and quantifying macromolecular interactions, neither method of them has any great advantage over the other [6].

The principle and application of the resonant mirror biosensor were described in 1993 [15,16]. The resonant mirror is integrated with the micro-cuvette device and permits to follow the optical phenomenon of an evanescent field. Changes in refractive index at the surface of the device, or the biological layer, change the angle at which light can be made to propagate in the waveguide: conditions for propagation are met at only one discrete angle (resonant angle). The change in angle is linear with respect to mass [17].

Interleukin-1 (IL-1) is a primary regulator of inflammatory and immune response, an important mediator in the pathogenesis of many inflammatory and immunologically mediated disease,

* Corresponding author. Tel.: +86 22 23506173; fax: +86 22 23506122.
E-mail address: qiangchen@nankai.edu.cn (Q. Chen).

0039-9140/$ – see front matter © 2005 Elsevier B.V. All rights reserved.
doi:10.1016/j.talanta.2005.12.036

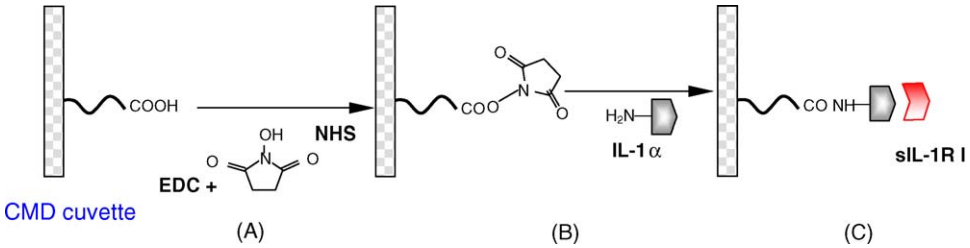

Fig. 1. Schematic diagram for IL-1α coupling to CMD cuvette surface. (A) EDC/NHS activation; (B) IL-1α bound on CMD cuvette by displacement of NHS; (C) sIL-1R I binding to immobilized IL-1α.

such as periodontal disease, and in the IL-1 family, there are three members, IL-1α, IL-1β and IL-1 receptor antagonist [18,19]. IL-1 activity can be due to IL-1α or IL-1β, as IL-1α and IL-1β bind to the same IL-1 receptor [20]. There are two types of IL-1 receptor, which can release from the cell surface in soluble form to become soluble IL-1 receptor (sIL-1R) I and sIL-1R II, respectively [21]. Previous evidences suggest that sIL-1R can block IL-1 activity [22,23], and is thought to be an effective regulator of the IL-1 signaling system [24]. At present the use of sIL-1R has become an important therapeutic approach for some disease mediated by IL-1. So the characters of affinity interaction between sIL-1R and IL-1 are essential for the development of sIL-1R in iatrology, medicine and clinical chemistry.

Here we have attempt to study the kinetic analysis of sIL-1R I binding to immobilized IL-1α in order to get a better insight and predict assay performance for the affinity interaction between sIL-1R I and IL-1α using an optical biosensor based on resonant mirror.

1. Materials and methods

1.1. Reagents

1-Ethyl-3-(3-dimethylaminopropyl) carbodiimide (EDC), *N*-hydroxysuccinimide (NHS) and ethanolamine were obtained from Shanghai Chemical Reagent Co., recombinant human IL-1α from Peprotech EC Co., and recombinant human sIL-1R I from R&D Co. Phosphate buffered saline/Tween-20 (PBST, pH 7.4) was composed of 0.01 M Na_2HPO_4/NaH_2PO_4, 0.138 M NaCl, 0.0027 M KCl and 0.05% Tween-20. All solutions were made by using deionized water. All reagents were of analytical grade and were used without further purification.

1.2. Instrument

All analyses were performed using a resonant mirror-based biosensor (Labsystems Affinity Sensors, Cambridge, UK). The exchangeable measuring dual-well cuvette has a carboxymethyl dextran (CMD) surface with a sensor area of 4 mm^2. This CMD cuvette surface is coated with an approximately 200 nm thick, low polydispersity CMD with approximately one carboxylate per two glucose residues, which enable the molecular (<1000 kDa) enter into the CMD matrix close to the surface, where the evanescent field is more intense. The CMD, a polymer of glucose residues with a low degree of branching, has been carboxymethylated to give carboxyl groups, which is coupled to protein primary amino groups (N-terminal and lysine residues) via EDC/NHS chemistry. Binding is measured in "arc seconds", corresponding to the accumulation of mass within the optical window at the binding surface, with a conversion of 163 arc seconds = 1 ng protein mm^{-2}. The protocol had been optimized on the optical biosensor with 0.4 s of data sampling interval, 25 °C of temperature, 100% of stirring rate in order to minimize mass transport effect.

1.3. Immobilization of IL-1α

CMD hydrogel on the cuvette was activated for 7–10 min by incubation with a 1:1 EDC/NHS mixture (0.1 M NHS and 0.4 M EDC). The function of the EDC/NHS is to activate and promote the formation of the covalent linkages by forming the *N*-hydroxysuccinimide ester. The carboxyl on the CMD bound NHS under the action of EDC and created active ester intermediate which bound the primary amines of the IL-1α to make amide bond. Thus, IL-1α was immobilized through its surface amine groups via amide bonds with the CMD. After washing with PBST, sIL-1R I was added and allowed to bind with immobilized IL-1α (Fig. 1).

1.4. Measure procedures

A measuring cycle of sIL-1R I binding to immobilized IL-1α consisted of the following steps.

(1) Recording the baseline in PBST on the CMD cuvette based on IL-1α.
(2) Adding sIL-1R I solution to record the association curve.
(3) Washing with PBST to record dissociation curve.
(4) Regenerating by 2 min incubation with 10 mM HCl.
(5) Washing with PBST to record the baseline for next cycle binding.

2. Results and discussion

2.1. Immobilization of IL-1α

Fig. 2 shows immobilization of IL-1α (600 nM) on the CMD cuvette surface. The light line indicated the control channel signal, which was reacted as the experiment channel, but without adding IL-1α. The control is important in order to follow non-specific binding phenomena or non-real binding signal on the biosensor surface. Unreacted NHS-esters in both assays were

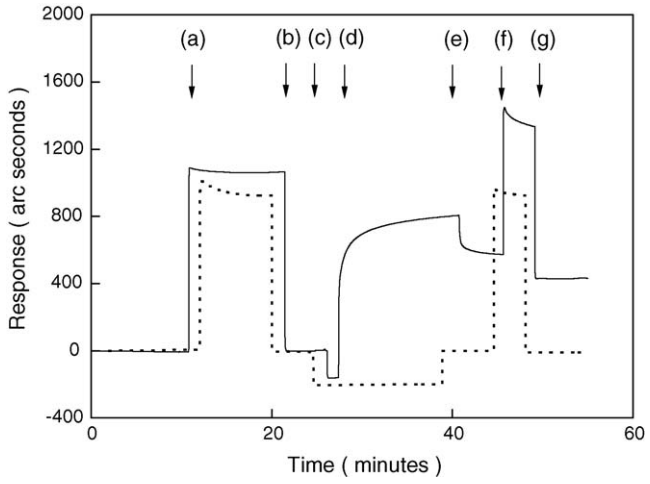

Fig. 2. Sensorgram of EDC/NHS activation and immobilization of IL-1α on CMD cuvette surface. Arrows indicate injections of (a) EDC/NHS mixture; (c) acetate; (d) IL-1α; (f) ethanolamine; (b), (e) and (g) PBST. The light line indicates the control channel signal.

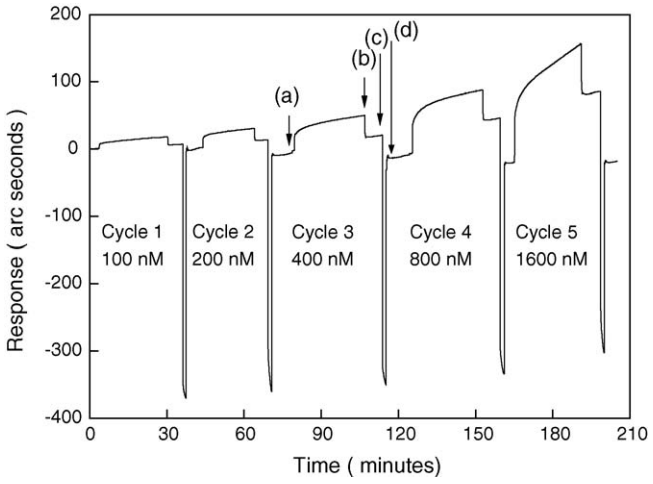

Fig. 4. Five cycles of different concentrations sIL-1RI binding to immobilized IL-1α. Arrows indicate injection of (a) sIL-1R I, (c) 10 mM HCl, (2) and (4) PBST.

blocked by incubation with 1 M ethanolamine. The actual immobilized amount of IL-1α was about 437.7 arc seconds after the complete washing. The surface concentration of the immobilized IL-1α on the CMD cuvette surface was calculated to be 2.69 ng mm^{-2}. Relative standard deviation (R.S.D.) was 3.1% ($n = 7$) for 600 nM of IL-1α immobilization on the CMD cuvette surface.

2.2. sIL-1R I binding to immobilized IL-1α

The cuvette based on IL-1α was rinsed three times by 50 μl PBST, then 50 μl of active and inactive sIL-1R I (800 nM) was added into the cuvette, respectively, and leaved to equilibrate for approximately 25 min (Fig. 3). The positive change in response was mainly due to sIL-1R I binding to immobilized IL-1α. At the end of this association, the reaction cuvette was washed with PBST and dissociation of the formed sIL-1R I–IL-1α complex was measured for 5–10 min. The immobilized amount of sIL-1R I was the one obtained immediately after adding PBST minus the start value before adding sIL-1R I, which was 48.7 arc seconds corresponding to immobilization of 0.30 ng mm^{-2} for active sIL-1R I binding to immobilized IL-1α, and no signal for inactive sIL-1R I.

The cuvette surface based on IL-1α was regenerated by incubation with 10 mM HCl for 2 min to strip sIL-1R I, then washed and re-equilibrated in PBST for next cycle of interaction between sIL-1R I and IL-1α. Fig. 4 depicts the individual binding curve for five given concentrations of sIL-1R I binding to immobilized IL-1α. From cycle 1 to cycle 5, the concentrations of sIL-1R I were 100, 200, 400, 800 and 1600 nM, respectively. As shown in Fig. 4, the response of interaction was linear with the concentration of sIL-1R I. The optical biosensor assay was completed in 30 min for one cycle of sIL-1R I binding to immobilized IL-1α and the same sensing surface was used repeatedly for the interaction analysis. R.S.D. varied from 1.7 to 2.6% ($n = 5$) for sIL-1R I binding to IL-1α in the sIL-1R I concentration range

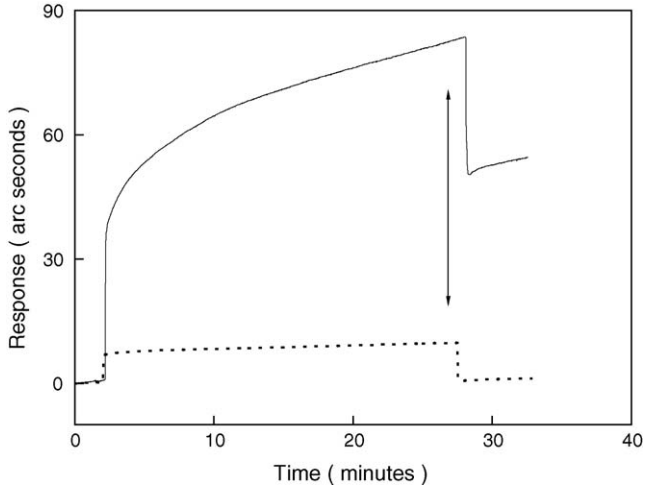

Fig. 3. Binding curves comparing the binding of active and inactive sIL-1R I to immobilized IL-1α. The arrow indicates the replacement of sIL-1R I with PBST. The light line indicates the control channel signal (inactive sIL-1R I).

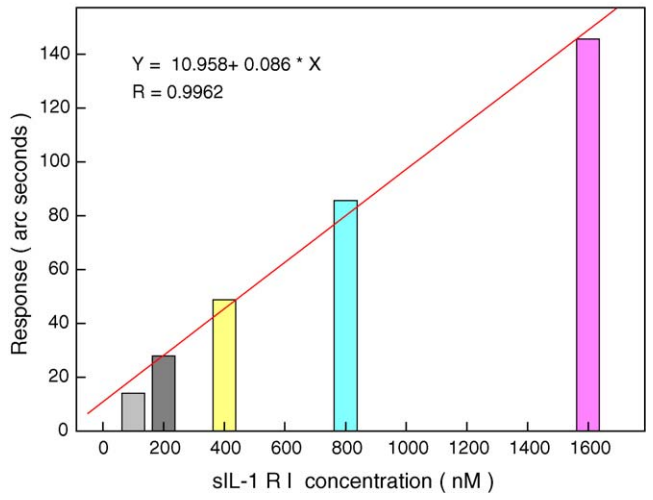

Fig. 5. Plots of response against corresponding concentration of sIL-1R I.

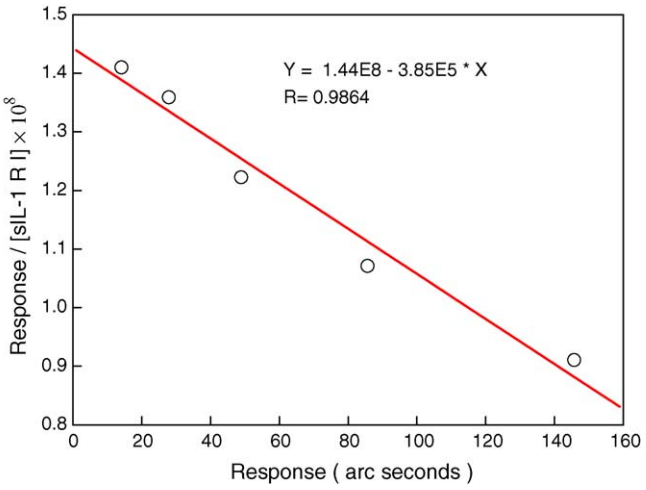

Fig. 6. Scatchard plot of sIL-1R I binding to IL-1α.

of 100–1600 nM. Fig. 5 shows the calibration curves for sIL-1R I with a range of 100–1600 nM in solution. The plot of response against corresponding concentration of sIL-1R I led to a linear dependence. Linear regression equation for sIL-1R I binding to immobilized IL-1α was Y (arc seconds) = 10.958 + 0.086 [sIL-1R I] nM (R = 0.9962). The determination of s IL-1R I in human serum sample was performed on the sensor utilizing standard addition method. The recovery was investigated by standard additions of s IL-1R I in the concentration range from 100 to 1600 nM to the human serum samples (n = 5), and the value of the recovery were in the range of 99.3–102.4%.

2.3. Equilibrium dissociation constant (K_D)

In order to characterize K_D for the interaction between sIL-1R I and IL-1α, the previously report approaches are adopted [25,26]. This analysis employs the equation:

$$\frac{R_{eq}}{[L]} = \frac{R_{max}}{K_D} - \frac{R_{eq}}{K_D}$$

where equilibrium data (R_{eq}) as obtained at fixed time of binding is the maximal response at a given sIL-1R I concentration. R_{max} represents the maximum response, occurring under conditions of sIL-1R I saturation with immobilized IL-1α, and K_D is the equilibrium dissociation constant of the interaction between sIL-1R I and IL-1α. So, a plot of $R_{eq}/[L]$ versus R_{eq} yields a line with the slope equal to $-1/K_D$. Fig. 6 shows the Scatchard plot of sIL-1R I binding to immobilized IL-1α on the CMD cuvette surface in the concentration range of 100–1600 nM of sIL-1R I (n = 7). The obtained linear regression equation for Scatchard plot within this range was $R_{eq}/[L] = 1.44 \times 10^8 - 3.85 \times 10^5\ R_{eq}$ (R = 0.9864). From this analysis, a K_D of 2.6×10^{-6} M was derived.

3. Conclusion

In this study an optical biosensor has been used to kinetic analysis of sIL-1R I binding to immobilized IL-1α, which appears to be a suitable and convenient tool. Compared to other binding assay such as ELISA, the optical biosensor allows to simplify the assay format and the time of analysis is reduced. As the affinity interaction between sIL-1R I and immobilized IL-1α is followed continuously in real time. Much more information is obtained about the interaction between sIL-1R I and immobilized IL-1α, which offers a principal advantage on the label-based methods, when only the end of the interaction is evaluated, and the repeated use of biosensor is quite promising. K_D of the interaction between sIL-1R I and immobilized IL-1α has been determined. So the assay is essential for the development of sIL-1R in iatrology, medicine and clinical chemistry, and it can provide principle and experiment data for the identification and filtration of their effective sIL-1R I antagonists.

Acknowledgement

The support by the National Science Foundation of China (Grant No. 90209054) is well acknowledged.

References

[1] P. Skladal, J. Braz. Chem. Soc 14 (2003) 491.
[2] J. Halamek, A. Makower, K. Knosche, P. Skladal, F.W. Scheller, Talanta 65 (2005) 337.
[3] L.R. leopoldo, M. Stefania, G. Alessandra, V. Stefania, R. Paolo, P.R. Roberto, Biosens. Bioelectron. 12 (1997) 765.
[4] X. Liu, D.Q. Song, Q.L. Zhang, Y. Tian, H.Q. Zhang, Talanta 62 (2004) 773.
[5] S. Toyama, K. Aoki, S. Kato, Sens. Actuators B 108 (2005) 903.
[6] L.D. Ward, D.J. Winzort, Anal. Biochem. 285 (2000) 179.
[7] D.G. Myszka, T.A. Morton, M.L. Doyle, I.M. Chaiken, Biophys. Chem. 64 (1997) 127.
[8] J. Tschmelak, G. Proll, G. Gauglitz, Talanta 65 (2005) 313.
[9] T. Arakawa, A. Kawbayashi, T. Saga, Sens. Actuators B 108 (2005) 899.
[10] M.I. Fisher, T. Tjarnhage, Biosens. Bioelectron. 15 (2000) 463.
[11] R.J. Green, R.A. Frazier, K.M. Shakesheff, M.C. Davies, C.J. Roberts, S.J.B. Tendler, Biomaterials 21 (2000) 1823.
[12] S. Hirmo, E. Artursson, G. Puu, T. Wadstrom, B. Nilsson, J. Microbiol. Meth. 37 (1999) 177.
[13] W.D. Wilson, Science 295 (2002) 2103.
[14] M. Minunni, S. Tombelli, M. Mascini, A. Bilia, M.C. Bergonzi, F.F. Vincieri, Talanta 65 (2005) 578.
[15] R. Cush, J.M. Cronin, W.J. Stewart, C.H. Maule, J. Molloy, N.J. Goddard, Biosens. Bioelectron. 8 (1993) 347.
[16] P.E. Buckle, R.J. Davies, T. Kinning, D. Yeung, P.R. Edwards, D. Pollard-Knight, Biosens. Bioelectron. 8 (1993) 355.
[17] A. Battaglia, C. Bertucci, E. Bombardelli, S. Cimitan, A. Guerrini, P. Morazzoni, A. Riva, Eur. J. Med. Chem. 38 (2003) 383.
[18] E. Stylianou, J. Saklatvala, Int. J. Biochem. Cell Biol. 30 (1998) 1075.
[19] Y. Kida, M. Kobayashi, T. Suzuki, A. Takeshita, Y. Okamatsu, S. Hanazawa, T. Yasui, K. Hasegawa, Cytokine 29 (2005) 159.
[20] C.A. Dinarello, Curr. Opin. Pharmacol. 4 (2004) 378.
[21] W.P. Arend, Cytokine Growth Factor Rev. 13 (2003) 323.
[22] W.C. Fanslow, J.E. Sims, H. Sassenfeid, P.J. Morrissey, S. Gillis, S.K. Dower, M.B. Widmer, Science 248 (1990) 739.
[23] K.C. Klasing, R.K. Peng, Dev. Comparat. Immunol. 25 (2001) 345.
[24] B. Sporri, M. Bickel, D. Dobbelaere, J. Machado, J.D. Lottaz, Cytokine Growth Factor Rev. 12 (2001) 27.
[25] G. Scathard, J.S. Coleman, C.A. Shen, J. Am. Chem. Soc. 79 (1957) 12.
[26] Y.P. Chang, Y.H. Chu, Anal. Biochem. 340 (2005) 74.